20. J. J. Mayerle, S. E. Denmark, B. V. Dephamphilis, J. A. Ibers, R. H. J. Holm, *J. Am. Chem. Soc.* **97**, 1032 (1975).
21. J. W. Peters, W. N. Lanzilotta, B. J. Lemon, L. C. Seefeldt, *Science* **282**, 1853 (1998).
22. M. W. W. Adams and E. I. Stiefel, *Science* **282**, 1842 (1998).
23. Pyruvate was identified by retention time using HPLC and GC-MS (after conversion to both its methyl and propyl derivatives). Pyruvate was not detected in any blank runs. Because of its better chromatographic resolution, GC-MS was used for quantitation of pyruvate yield; the total ion current was calibrated with solutions containing known quantities of derivatized pyruvate.
24. This research was carried out under the auspices of the NASA Astrobiology Institute under NASA Cooperative Agreement NAI NCC2-1056. We thank J. Brandes, M. Fogel, and M. McCarthy for insightful discussions and H. Yang and J. Adler for x-ray diffraction data collection.

16 May 2000; accepted 5 July 2000

Galileo Magnetometer Measurements: A Stronger Case for a Subsurface Ocean at Europa

Margaret G. Kivelson,* Krishan K. Khurana, Christopher T. Russell, Martin Volwerk, Raymond J. Walker, Christophe Zimmer

On 3 January 2000, the Galileo spacecraft passed close to Europa when it was located far south of Jupiter's magnetic equator in a region where the radial component of the magnetospheric magnetic field points inward toward Jupiter. This pass with a previously unexamined orientation of the external forcing field distinguished between an induced and a permanent magnetic dipole moment model of Europa's internal field. The Galileo magnetometer measured changes in the magnetic field predicted if a current-carrying outer shell, such as a planet-scale liquid ocean, is present beneath the icy surface. The evidence that Europa's field varies temporally strengthens the argument that a liquid ocean exists beneath the present-day surface.

Europa, one of the icy moons of Jupiter, may have a layer of liquid water beneath its surface. Features of Europa's tortured surface revealed by Galileo's imaging system may have formed as its surface ice stretched, broke, and rearranged itself while floating on a watery subsurface sea (*1–4*). But even if water shaped the surface we see today, it may have frozen hundreds of thousands of years ago. Those searching for possible abodes of life elsewhere in the solar system would like to know whether water exists beneath the surface at the present epoch.

In the initial report (*5*), the magnetic perturbations measured on Galileo's first pass by Europa were characterized as the signature of an internal dipole moment. The Galileo magnetometer team subsequently reported (*6*, *7*) that many features of their data on close passes by Europa in 1996 and 1998 can be modeled as the electromagnetic response to Jupiter's time-varying magnetospheric magnetic field if a layer of electrically conducting material exists near Europa's surface. Although the dominant, southward-oriented magnetic field imposed by Jupiter's magnetosphere at Europa's position is about constant, the projection of the magnetospheric field into Europa's equatorial plane varies with the synodic period (Jupiter's rotation period, 11.2 hours as seen from Europa) and has a mean value close to zero. Such a time-varying magnetic field, referred to as the primary field, can drive inductive currents through an electrical conductor. Inductive currents, in turn, generate a secondary field, whose source can be represented as a time-varying magnetic dipole moment lying in Europa's equatorial plane with an orientation approximately antiparallel to the instantaneous orientation of the primary field (*8*, *9*). If one models Europa as an idealized, highly conducting sphere (conductivity $\gg 1$ S m^{-1}) of radius 1 R_E (radius of Europa = 1560 km) and if the primary field ($B_x(t)$, $B_y(t)$, B_z) is uniform over the scale of Europa, then the components (*10*) of the induced magnetic moment (**M**) are $-1/2(B_x(t), B_y(t), 0)$ in magnetic field units, implying that at the surface of Europa, the radial components of the induced field and the time-varying primary field cancel. Table 1 gives values of this idealized induced dipole moment at the time of closest approach (labeled "Ind") and other key parameters of all Europa passes for which the magnetometer acquired data (E4, E11, E12, E14, E15, E17, E19, and E26). We shall focus hereafter only on passes that came within 2000 km of Europa's surface (E4, E12, E14, E19, and E26) for which the signatures of internal sources can have amplitudes large enough to be clearly detected (*11*).

The idealized induction model is consis-

Institute of Geophysics and Planetary Physics, University of California, Los Angeles, CA 90095–1567, USA.

*To whom correspondence should be addressed. E-mail: mkivelson@igpp.ucla.edu

Table 1. Idealized induced dipole moment at closest approach and key parameters of Europa passes. Fitted int, fitted interval; Mag lat and SIII long, System III latitude and longitude; CA, closest approach above Europa's surface; Europa lat and E-long, Europacentric latitude and longitude measured eastward; Bf, best-fit (or measured) dipole model; Ind, induced dipole model.

	E4		E11		E12		E14	
Date	19 December 1996		6 November 1997		16 December 1997		29 March 1998	
Fitted int (UT)	06:32–07:10		20:30–21:00		11:45–12:15		13:05–13:40	
Mag lat (°)	6.5		8.7		−0.8		9.2	
SIII long (°)	157		223		118		184	
CA altitude (km)	688		2039		196		1649	
Europa lat (°)	−1.6		26		−8.6		12	
Europa E-long (°)	322		219		134		131	
	BF	Ind	BF	Ind	BF	Ind	BF	Ind
M_x (nT)	8	−27	−7	21	−61	−39	−16	−5
M_y (nT)	97	88	−25	96	14	16	160	108
M_z (nT)	−52	0	−122	0	392	0	167	0
	E15		E17		E19		E26	
Date	31 May 1998		26 September 1998		1 February 1999		3 January 2000	
Fitted int (UT)	21:12–21:30		03:40–04:20		02:00–02:38		17:45–18:15	
Mag lat (°)	−0.5		3.8		4.8		−9.6	
SIII long (°)	293		138		256		2	
CA altitude (km)	2519		3588		1444		373	
Europa lat (°)	14.9		−42.5		31.0		−46.4	
Europa E-long (°)	225		220		29		83	
	BF	Ind	BF	Ind	BF	Ind	BF	Ind
M_x (nT)	−65	33	152	−38	108	33	−42	11
M_y (nT)	−107	−18	269	47	−12	39	−126	−104
M_z (nT)	−278	0	−496	0	192	0	83	0

tent with the orientation and the magnitude of the equatorial dipole moment observed on the close Europa passes on Galileo's fourth and fourteenth orbits around Jupiter (referred to as E4 and E14; data plotted in Figs. 1 and 2).

Although measurements from the E4 and E14 passes were consistent with perturbations arising from inductive currents, one could not exclude the possibility that a permanent dipole moment tilted toward the *y* axis was the source of the observed magnetic perturbations. Both passes occurred in Jupiter's northern magnetic hemisphere at times when the magnetospheric field at Europa pointed away from Jupiter and therefore the induced dipole moment pointed toward Jupiter. However, an induced equatorial dipole moment changes orientation and amplitude over a synodic period in a predictable manner. Consequently, a flyby in the southern magnetospheric hemisphere in the opposite phase of the driving signal would test the validity of the model by determining whether Europa's inferred magnetic moment is or is not variable. The inset in Fig. 3 shows the variation of the *x* and *y* components of Jupiter's magnetospheric field at Europa over a synodic period (*12*). Also marked are the values of these components at closest approach to Europa for the passes at altitudes <2000 km. The E26 encounter (3 January 2000) (see data plotted in Fig. 4) was designed to occur when Europa was in the southern magnetospheric hemisphere and the driving field was almost 180° out of phase with its value on the E4 and E14 passes. In this situation, Europa's equatorial dipole moment would point away from Jupiter if it were induced but would remain pointing toward Jupiter if it were quasi-static.

The best-fit dipole moment (*13*) and the idealized induced dipole moment track each other relatively closely and represent the changes on the scale of Europa's diameter. (Table 1 provides the components of these dipole moments for all passes.) In contrast, the signature that would have been observed on E26 if the dipole moment had been that fitted to the E4 data (moment pointing toward Jupiter) is at variance with the measurements. This reveals unambiguously that the orientation of the equatorial dipole moment changed.

Although the modeled signature of an inductive dipole moment tracks the data (Figs. 1, 2, and 4) fairly well, there are discrepancies. By understanding how plasma currents contribute to the field perturbations, one can identify the components that reveal most about the internal sources of the magnetic perturbations. The effect of currents coupling Europa's environment to Jupiter's ionosphere, referred to as Alfvén wing currents, are well understood (*14*, *15*). These currents roughly align with the background field north and south of Europa, and

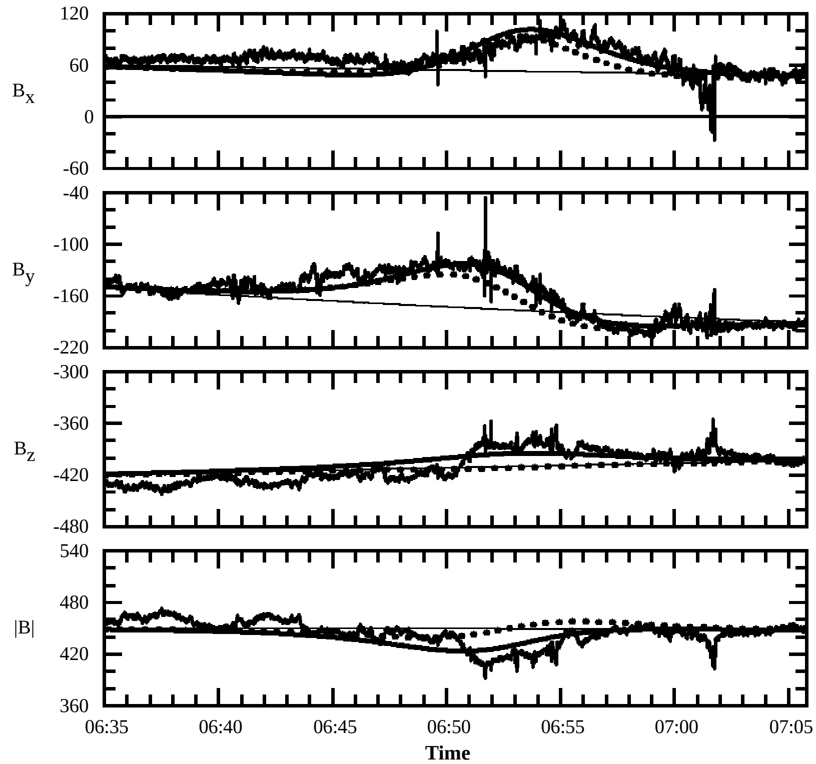

Fig. 1. Magnetometer data in the EphiO (*10*) coordinate system (three components and the field magnitude in nT) from pass E4 on 19 December 1996 plotted against spacecraft event time in UT for a range of ~4 R_E from Europa's center. The solid curves are data points. The slowly changing thin curves, obtained from a polynomial fit to the field components measured before and after the encounter, represent the background field without Europa perturbations. The dotted curves are predictions from the induced dipole model without plasma effects. The heavy solid curves are the least squares fits to a tilted dipole moment, referred to in the text as the measured magnetic moment.

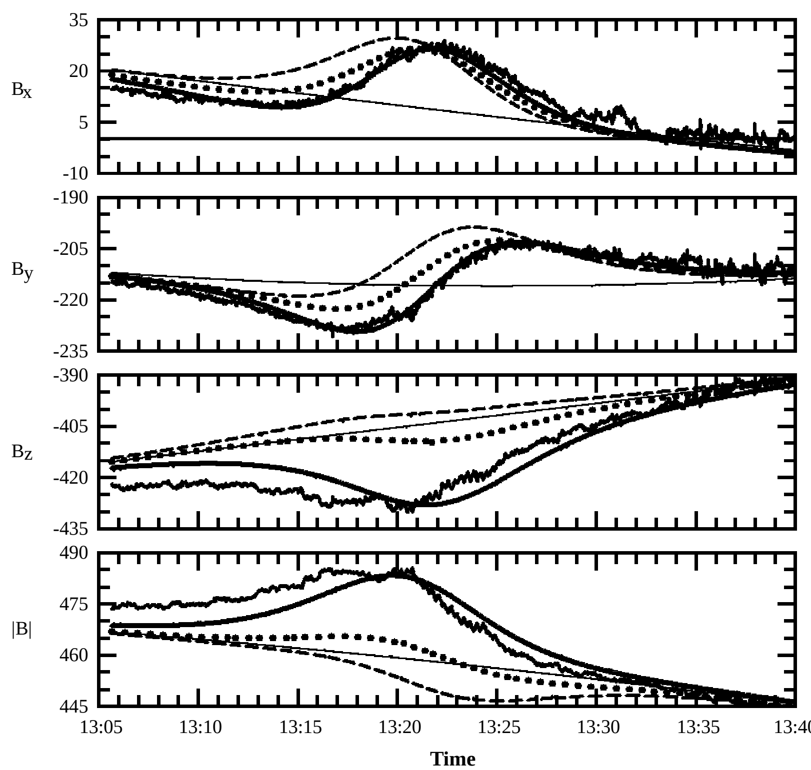

Fig. 2. The E14 pass on 29 March 1998 showing data within 5 R_E of Europa's center. Curves are as in Fig. 1 with addition of the dashed curves, which represent the values along this orbit from the fitted E4 dipole moment.

they close through Europa or its ionosphere and through currents produced by ionization of neutral species in the surrounding plasma. The Alfvén wing currents bend the background field in the direction of the flow and the closure currents affect the field magnitude near Europa, increasing it upstream and decreasing it downstream. Bending produces a negative change in B_x north of Europa and a positive change south of Europa. The field may also bulge around Europa producing perturbations in B_y, which are generally smaller than those in B_x. Away from Europa's equator (Table 1), the Alfvén wing perturbation may contaminate the signature of internal sources in the *x* and *y* components of the field. It may also produce fluctuations of the field components comparable in magnitude to the perturbations estimated for an idealized induced response over distances shorter than 1 R_E [e.g., E26, Fig. 4; E12, Web fig. 1 (*16*); and E19, Web fig. 2 (*16*)]. However, on near equatorial passes (E4 and E14), Alfvén wing currents contribute little to B_x or B_y but do affect B_z. Fortunately, near the equator, an induced dipole moment (which lies in the *x-y* plane) contributes only to the B_x and B_y components. Thus, the close correspondence between the model and the data for these components on the low-latitude passes is meaningful. Away from the equator (passes E19 and E26), all components (but particularly B_x) may be affected by Alfvén wing currents. For example, B_x is modified by the negative (positive) contribution of the Alfvén wing bendback on the E19 pass north of the equator (E26 pass south of the equator). This accounts for part of the discrepancy between the data and the induced field model [Fig. 4 and Web fig. 2 (*16*)]. Pass E12 occurred close to the center of the jovian current sheet, where exceptionally strong pickup produced unexpectedly large perturbations over many R_E (the field near closest approach was double the background field in magnitude). The large error of fit to a dipole moment (Fig. 3) reveals that currents external to Europa dominate these measurements.

Because M_y is the largest component of the induced (time-varying) magnetic moment and the one least modified by plasma effects for the low latitudes passes, we focus on its measured values. The measured M_y and the M_y from the induced field model vary in phase with each other if the dipole moments are produced by induction. Figure 3 shows that the modeled and measured moments track one another within experimental uncertainty. The critical aspect of Fig. 3 is that if the dipole moment were permanent, the measured M_y on E26 would have been the same as it was on E4 and E14 within the uncertainty of the data fits; it would have appeared in the upper left quadrant instead of the lower left quadrant, as predicted by the inductive model.

Europa's response to the changing magnetic field at its orbit (inset to Fig. 3) has been modeled as that of a perfectly conducting sphere responding to a uniform time-varying primary field. Alfvén wing perturbations are also time varying but their nonuniform structure contributes only to internal spherical harmonics of higher than dipole order (*17*). Nonetheless, there is harmonic aliasing in any fit to data acquired along a spacecraft trajectory rather than everywhere on a closed surface. Alfvén wing currents do, therefore, contribute to the best-fit dipole moment.

A spherical shell conductor with 1 R_E outer radius would produce nearly the same signature as a sphere of the same size for sufficiently high conductivity (*7*). For example (*18*, *19*), the amplitude of the response of

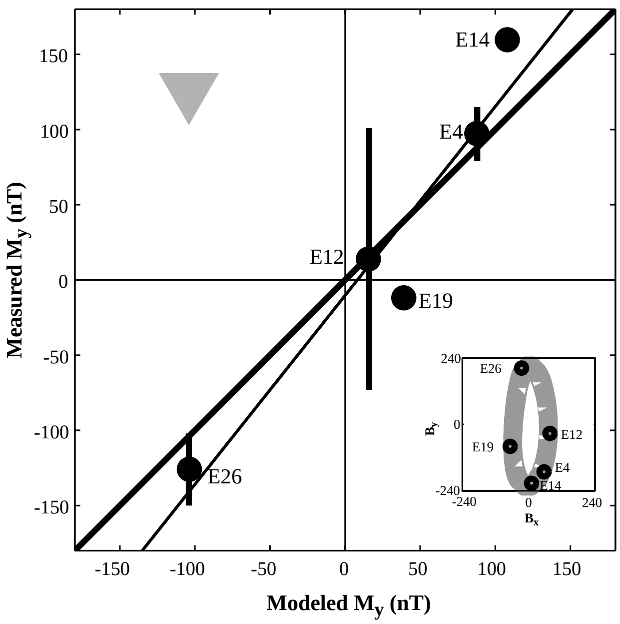

Fig. 3. The radial (positive toward Jupiter) component of the equatorial dipole moment fitted to the observed data plotted against predictions for a 1 R_E highly conducting sphere (the induced model). The heavy line represents the model. The narrow line is a least squares fit to the data. Error bars give the error of fit for the best-fit dipole. Estimates of the contributions of plasma currents have not been removed. The critical test occurred on E26. If the dipole moment fitted to E4 and E14 had been permanent, the point would have fallen at the approximate position of the triangle in the upper left-hand quadrant. (Inset) Variation over Europa's synodic period of the B_x and B_y components of Jupiter's magnetospheric field at Europa's location. Dots show the values observed at closest approach to Europa on the relatively close encounters. Time increases clockwise.

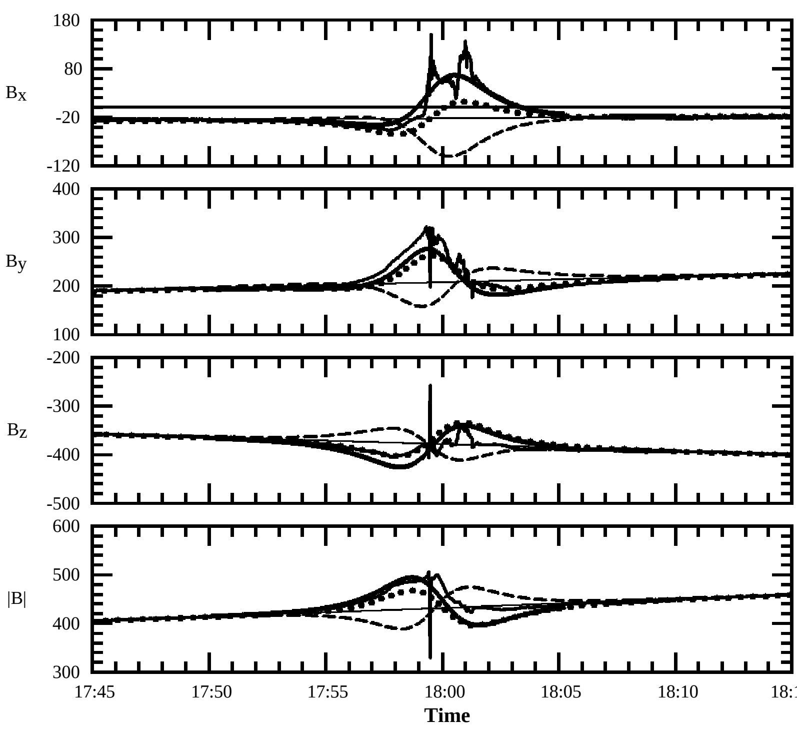

Fig. 4. The E26 pass on 3 January 2000: data within 5 R_E from Europa's center. Curves are as in Fig. 2. The dashed curves computed from the dipole moment fit to the E4 pass are in antiphase to both the dipole fitted to the E26 data (heavy solid curves) and to the inductive response model (dotted curves).

a spherical shell of ~7.5-km depth below Europa's surface and a conductivity of 2.75 S m^{-1} for Earth's oceans (*20*) would be 90% that of a highly conducting sphere with a phase lag relative to the primary field of 25°. The amplitudes of the induced magnetic moment for E4, E14, and E26 would be reduced by the phase lag (*21*). If the ocean were thicker, but still close to the surface, or if the conductivity were higher, the phase lag would decrease, and the amplitude of the response would increase.

On passes E4, E12, E14, E19, and E26, currents induced by the time-varying primary field in a Europan ionosphere may contribute to the magnetic perturbation. Elsewhere (*18*), we have calculated the signature of induced currents flowing above the surface, close to Galileo's trajectory, in a conducting shell of larger than 1 R_E radius. Based on the measured ionospheric density and scale height (*22*) and measured (*23*) or modeled (*24*) atmospheric properties, we find that ionospheric currents fail to account for the observations by an order of magnitude.

The case for a subsurface electrical conductor on a planetary-wide scale passed the test of the E26 flyby with flying colors. Although the electrically conducting layer need not be salty water, water is the most probable medium on Europa. Geological evidence has been interpreted as consistent with surface effects of subsurface liquid water, but the defining features could have been formed in the distant past. The magnetometer result makes it likely that liquid water persists in the present epoch.

References and Notes

1. R. Greeley *et al.*, *Icarus* **135**, 25 (1998).
2. R. T. Pappalardo, J. W. Head, R. Greeley, *Sci. Am.* **281**, 54 (1999).
3. G. V. Hoppa, B. R. Tufts, R. Greenberg, P. E. Geissler, *Science* **285**, 1899 (1999).
4. R. Greenberg *et al.*, *Icarus* **141**, 263 (1999).
5. M. G. Kivelson *et al.*, *Science* **276**, 1239 (1997).
6. K. K. Khurana *et al.*, *Nature* **395**, 777 (1998).
7. M. G. Kivelson *et al.*, *J. Geophys. Res.* **104**, 4609 (1999).
8. D. S. Colburn and R. T. Reynolds, *Icarus* **63**, 39 (1985).
9. F. M. Neubauer, *J. Geophys. Res.*, **103**, 19843 (1998).
10. The coordinate system used in this paper (referred to as Ephio) is Europa-centric with *x* along the corotating plasma flow, *y* radially in toward Jupiter, and *z* parallel to Jupiter's spin axis. In conventional units of A m^2, the magnetic moment is $4\pi R_E^3 \mathbf{M}/\mu_o$, where μ_o is the magnetic permeability.
11. Our rationale for ignoring passes at altitude greater than 2000 km is that at 2000-km altitude and directly over the induced magnetic pole, the signal from an internal magnetic moment of ~100 nT (see E11, Table 1) is less than 8.4 nT. Away from the pole, the signal amplitude becomes even smaller. Such small amplitude signals are difficult to interpret given the levels of fluctuations typical of the plasma background.
12. The components of the magnetospheric field are plotted with a broad line to take into account variations of the primary field that occur at other than the synodic period. Such variations are expected because Europa's radial distance and latitude vary from pass to pass as a result of the ellipticity and slight inclination of Europa's orbit and because of temporal variations in the plasma sheet.
13. The measured magnetic moment is obtained by fitting the difference between the measured field components and the smoothly varying background field to a dipole field over the intervals tabulated in Table 1. The components of the dipole moment are obtained by a least squares technique.
14. F. M. Neubauer, *J. Geophys. Res.* **85**, 1171 (1980).
15. D. J. Southwood, M. G. Kivelson, R. J. Walker, J. A. Slavin, *J. Geophys. Res.* **85**, 5959 (1980).
16. Web figures 1 and 2 are available at Science *Online* at www.sciencemag.org/feature/data/1052679.shl.
17. F. M. Neubauer, *J. Geophys. Res.* **104**, 28671 (1999).
18. C. Zimmer, K. K. Khurana, M. G. Kivelson, *Icarus*, in press. This work used the electromagnetic induction solution for multiple concentric shells given in (*19*).
19. W. D. Parkinson, *Introduction to Geomagnetism* (Elsevier, New York, 1983), p. 313.
20. R. B. Montgomery, in *American Institute of Physics Handbook*, D. E. Gray, Ed. (McGraw-Hill, New York, 1963), pp. 125–127.
21. This can be understood by noting that in the inset to Fig. 3, the primary field was increasing in the hour before each of those encounters. Thus, a phase lag of 25° or 0.6 hours implies that the induced currents are responding to a smaller primary field.
22. A. J. Kliore, D. P Hinson, F. M. Flasar, A. F. Nagy, T. E. Cravens, *Science* **277**, 355 (1997).
23. D. T. Hall, P. D. Feldman, M. A. McGrath, D. F. Strobel, *Astrophys. J.* **499**, 475 (1998).
24. J. Saur, D. F. Strobel, F. M. Neubauer, *J. Geophys. Res.* **103**, 19947 (1998).

25. We are grateful to our programmers, S. Joy and J. Mafi, for their devoted efforts to acquire and process the data on a short time scale and during holiday periods. Support for this work was provided in part by contract JPL 958694 from NASA's Jet Propulsion Laboratory (JPL), which manages the Galileo mission. Special thanks are due to D. Bindschadler, C. Polanskey, J. Erickson, and others at JPL who worked to design a Europa pass optimized to provide the test that we report here.

31 May 2000; accepted 10 July 2000

Molecular Analysis of Plant Migration and Refugia in the Arctic

Richard J. Abbott,[1]* Lisa C. Smith,[1] Richard I. Milne,[1] Robert M. M. Crawford,[1] Kirsten Wolff,[1,2] Jean Balfour[1]

The arctic flora is thought to have originated during the late Tertiary, approximately 3 million years ago. Plant migration routes during colonization of the Arctic are currently unknown, and uncertainty remains over where arctic plants survived Pleistocene glaciations. A phylogenetic analysis of chloroplast DNA variation in the purple saxifrage (*Saxifraga oppositifolia*) indicates that this plant first occurred in the Arctic in western Beringia before it migrated east and west to achieve a circumpolar distribution. The geographical distribution of chloroplast DNA variation in the species supports the hypothesis that, during Pleistocene glaciations, some plant refugia were located in the Arctic as well as at more southern latitudes.

Throughout much of the Tertiary, the Arctic supported continuous forests (*1, 2*). Only toward the end of this period does fossil evidence show that certain present-day arctic plants were established and widely distributed in the Arctic, although extensive areas of lowland tundra were absent (*3, 4*). Many arctic plants are thought to have originated in the high mountain ranges of central Asia and North America (*1, 5, 6*), to have spread northward to the Arctic as global temperatures fell in the late Tertiary, and to have achieved a circumpolar distribution by the late Tertiary to early Pleistocene (*5*). However, phytogeographic and fossil evidence to support these proposals is either lacking or fragmentary. Consequently, the migration routes followed by plants during the early colonization of the Arctic remain unknown.

During the Pleistocene, the distribution and ranges of arctic plants were greatly affected by the advance and retreat of ice sheets, and it was initially supposed that their survival depended on migration southward, ahead of advancing ice sheets (*7*). However, since the discovery that large parts of the Arctic and Subarctic in northwest America and eastern Siberia (i.e., Beringia) were never glaciated (*5, 8, 9*), these northern areas are also thought to have served as important refugia for arctic plants during Pleistocene glaciations (*5*).

We surveyed chloroplast DNA (cpDNA) variation throughout a large part of the distribution of the circumpolar arctic-alpine plant, *Saxifraga oppositifolia* (purple saxifrage). This is a long-lived, perennial, herbaceous, and outcrossing plant (*10*) that is distributed throughout the Arctic and in mountain ranges to the south (*11*). Both diploid and

[1]Division of Environmental and Evolutionary Biology, Harold Mitchell Building, School of Biology, University of St. Andrews, St. Andrews, Fife KY16 9TH, UK. [2]Department of Agricultural and Environmental Sciences, Ridley Building, University of Newcastle, Newcastle-upon-Tyne NE1 7RU, UK.

*To whom correspondence should be addressed. E-mail: rja@st-and.ac.uk